

Density of states of interacting quantum wires with impurities: a Dyson equation approach

R. Zamoum¹, M. Guigou^{2,3}, C. Bena^{2,3}, and A. Crépieux¹

¹*Aix Marseille Université, Université de Toulon,
CNRS, CPT UMR 7332, 13288 Marseille, France*

²*Institut de Physique Théorique, CEA/Saclay, Orme des Merisiers, 91190 Gif-sur-Yvette Cedex, France and*

³*Laboratoire de Physique des Solides, UMR 8502, Bât. 510, 91405 Orsay Cedex, France*

We calculate the density of states for an interacting quantum wire in the presence two impurities of arbitrary potential strength. To perform this calculation, we describe the Coulomb interactions in the wire within the Tomonaga-Luttinger liquid theory. After establishing and solving the Dyson equation for the fermionic retarded Green's functions, we study how the profile of the local density of states is affected by the interactions in the entire range of impurity potentials. Same as in the non-interacting case, when increasing the impurity strength, the central part of the wire becomes more and more disconnected from the semi-infinite leads, and discrete localized states begin to form; the width of the corresponding peaks in the spectrum depends on the interaction strength. As expected from the Luttinger liquid theory, impurities also induce a reduction of the local density of states at small energies. Two other important aspects are highlighted: the appearance of an extra-modulation in the density of states at non-zero Fermi momentum when interactions are present, and the fact that forward scattering must be taken into account in order to recover the Coulomb blockade regime for strong impurities.

PACS numbers:

I. INTRODUCTION

The interplay between interactions and disorder is a long-standing problem in condensed matter physics. In one-dimensional systems, in which the interactions can be treated exactly using the Luttinger liquid theory¹⁻³ and bosonization,^{4,5} a lot of progress to understand the effects of impurities has been made over the last twenty years. It was shown that repulsive interactions like the Coulomb interactions renormalize the impurity strength, such that at low energy even a weak impurity has a very strong effect and can cut the wire into two pieces.⁶⁻⁹ This translates into a reduction of the local density of states (LDOS) at low energies, and the LDOS decays to zero as a power-law.¹⁰⁻¹⁴ At high energies the effect of the impurity consists in a small power-law correction of the unperturbed LDOS. The two power-laws are characterized by two different exponents which depend on the interaction strength.

These two regimes have been described perturbatively by various techniques, such as the renormalization group¹⁵ and Keldysh formalism.^{13,14} These techniques have as starting point either the infinite clean wire, or a system of two decoupled semi-infinite wires, and one focused on the small perturbations around these points induced by the impurities. However, the transition between the two limits cannot be captured by perturbative techniques, and special techniques such as the Bethe ansatz are necessary.¹⁶ It would be thus of great interest to be able to capture this transition by more direct methods such as the Dyson equation technique we propose here. This is our first motivation to tackle this problem.

Our second motivation comes from a more applied perspective, and consists in providing a method to disen-

tangle the effects of the metallic contacts which are inevitably connected to an interacting quantum wire (QW) in the measurement process, allowing one to have access to the interacting physics in the wire and eventually evaluate the strength of the interactions therein. The first attempts to measure the interaction parameters in a QW rely on the existence of the impurity-induced power-law corrections in the LDOS detectable in conductance measurements.^{9,17} However, this has turned to be a very difficult task, due especially to the incertitudes in fitting power-law dependences over small intervals of energies. Subsequently, other more direct measurements such as the shot noise have been proposed.¹⁸⁻²² Unfortunately, it was shown that in such experiments, the metallic contacts prevent one from having access to the value of the interacting parameter.^{14,19,23-25}

The modelization of the metallic contacts provide us with two challenges. The first consists in the introduction of two impurities at the two junctions between the wire and the contacts. In general, the impurity potentials induced by these impurities are neither too small nor too large, and a non-perturbative technique would be required to capture the transition between small and large values of the impurity potential. Secondly, the physics of the system is greatly affected by the fact that the two semi-infinite metallic leads are non-interacting, and thus a correct modelization of the system needs to include the spatial inhomogeneity in the interaction strength. As mentioned above, this inhomogeneity is what blocks one from having access to the value of the interacting parameter via shot noise experiments. These two aspects need to be taken into account to correctly evaluate the effect of the contacts.

The first issue, i.e. the transition between the small

and large impurities is an interesting problem which is present even in the absence of interactions. For a non-interacting system it has been shown that a transition from a Fabry-Perot to a Coulomb-blockade regime occurs when the impurity strength increases. Thus, for weak impurities, Fabry-Perot oscillations arise in the dependence of the LDOS on energy.^{23,26–28} For large values of the impurity potential the system is cut into a central quantum-dot like region plus two semi-infinite wires, and the energy spectrum of the central part consists in discrete levels whose energy is proportional to its inverse length.^{29–33} The width of these states becomes smaller and smaller when the central part is more and more disconnected from the leads.

Understanding the effect of the interactions on the transition between the Coulomb blockade and the Fabry-Perot regime is a long-standing mesoscopic physics problem. Various other factors also come into place, such as lifting the degeneracy between the energy levels when the Coulomb interactions are present. This is especially interesting in the spinful case, in this situation the periodicity of oscillations in the LDOS is expected to change between the Coulomb blockade and the Fabry-Perot regimes; various works have been trying to approach this problems using different methods.^{34,35}

In this work we develop a new approach that allows one to study the interplay between impurities and interactions for arbitrary size impurities. Our approach is based on writing down and solving the Dyson equations for a wire with one or two impurities. In the present paper we consider an infinite homogeneous interacting QW and the corresponding form for the fermionic Green's functions. This allows us to study the first aspect of the problem raised by the presence of the contacts, i.e. the presence of one or two impurities of arbitrary size.

We start with the study of a infinite homogeneous interacting QW with a single impurity. We calculate the form of the Friedel oscillations as well as the dependence of the LDOS with energy. For weak impurities we retrieve the expected Luttinger liquid power-law dependence of the impurity with energy at both low and high energies. For strong impurities at either high energies or large distances to impurity, we recover a power-law dependence with the same exponent $(K + 1/K - 2)/2$ as for the weak-impurity regime, consistent with the Luttinger liquid predictions. However, at low energy and small distance our approach fails to recover the transition to a different power-law exponent characteristic to breaking the wire into two independence pieces $(1/K - 1)$. We think that this comes from a drawback in the approximation in our formalism, which is neglecting the interactions between the electrons on the right and on the left of the impurity. This nevertheless does not affect the behavior at large distances/energies, and the validity of the main results of this paper, i.e. the dependence of the LDOS in a wire with two impurities and the transition from the weak-impurity regime to the strong-impurity regime in this limit.

To improve this approximation so that we can have access to all the energy scales of the problem, we plan in the future to focus on an inhomogeneous wire made of a central finite-size interacting region and two semi-infinite leads. Thus, by construction there can be no interacting terms between the electrons on the right and left of the impurities, so our approximation will be fully valid for this system. We can use the Dyson equation method presented here also for this system, its fermionic Green's function being calculated in closed form.³⁶

Moreover this system is more interesting since it models a realistic system in the presence of metallic contacts. This will allow us in the future to tackle the second aspect of our problem, which is the spatial inhomogeneity in the interaction strength. We can also generalize our approach to take into account other factors such as the electronic spin, this will allow us to characterize more realistic system and make contact with experiments.

For an homogeneous interacting wire with two impurity, we find that the main effect of interactions is to modify the amplitude of the Fabry-Perot oscillations, as well as of the height and width of the Coulomb blockade peaks. Thus the oscillations are reduced in the presence of interactions, while the peaks get wider and smaller when interactions are taken into account. The interactions do not affect the periodicity of the oscillations, neither the distance between the peaks. Moreover, same as for a single impurity, power-law dependences of the LDOS with energy arise, and the LDOS is reduced to zero on the impurity sites.

Another confirmation of the validity of our approach at large distance and high energy is the agreement between the form that we obtain for the LDOS in a wire with two impurities, and that obtained via a complete different technique by Anfuso and Eggert in Ref. 37 for a Luttinger in a box. Same as Ref. 37 we find that at non-zero Fermi momentum there is an extra modulation in the space dependence of the LDOS which arises solely in the presence of interactions.

The paper is organized as follows: we present the model in section II, and the general solution to the Dyson equations for an arbitrary chiral wire with one or two impurities in section III. In section IV, we study the simple situation of a wire with a single impurity. In Section V, we discuss the results for an infinite homogeneous wire with two impurities. We conclude in section VI.

II. MODEL

We consider a one-channel interacting QW with two impurities at positions $x_{1,2} = \pm L/2$ (see Fig. 1), where L is the distance between the impurities. The impurities are described by backward scattering potentials $\lambda_{1,2}^B$ and forward scattering potentials $\lambda_{1,2}^F$. The Hamiltonian can be written as $H = H_0 + H_{\text{int}} + H_{\text{imp}}$, where H_0 describes

the non-interacting QW without impurities:

$$H_0 = -i\hbar v_F \sum_{r=\pm} r \int_{-\infty}^{\infty} \psi_r^\dagger(x) \partial_x \psi_r(x) dx, \quad (1)$$

with v_F is the Fermi velocity, ψ_r^\dagger and ψ_r are the creation and annihilation fermionic operators associated to the right movers ($r = +$) and left movers ($r = -$). The Hamiltonian H_{int} describes the Coulomb interaction in the wire:

$$H_{\text{int}} = \frac{1}{2} \int_{-\infty}^{\infty} \int_{-\infty}^{\infty} \hat{\rho}(x) V(x, x') \hat{\rho}(x') dx dx', \quad (2)$$

where $\hat{\rho}(x) = \sum_{r,r'} \psi_r^\dagger(x) \psi_{r'}(x)$ is the density operator, and V is the Coulomb potential. The impurity Hamiltonian contains two types of contribution $H_{\text{imp}} = H_B + H_F$, backward scattering

$$H_B = \sum_{r=\pm} \sum_{i=1,2} \int_{-\infty}^{\infty} \lambda_i^B(x) \psi_r^\dagger(x) \psi_{-r}(x) dx, \quad (3)$$

and forward scattering

$$H_F = \sum_{r=\pm} \sum_{i=1,2} \int_{-\infty}^{\infty} \lambda_i^F(x) \psi_r^\dagger(x) \psi_r(x) dx. \quad (4)$$

In the following, we assume that the impurities are localized, i.e. $\lambda_i^{F,B}(x) = \Gamma_i^{F,B} \delta(x - x_i)$. Notice that in some works dealing with impurities in a Luttinger liquid, the forward scattering terms were not included with the justification that such terms could be incorporated in the kinetic part.³⁸⁻⁴¹ This is correct in the weak-impurity limit but does not hold in the strong-impurity limit. Indeed, the density of states is strongly affected by the forward scattering terms at strong $\Gamma_{1,2}^{F,B}$; these terms need to be taken into account explicitly in order to recover the Coulomb blockade regime.

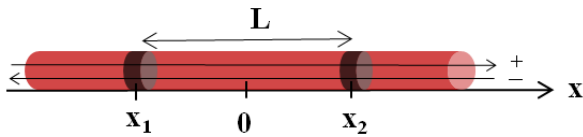


FIG. 1: One dimensional wire with two impurities located at positions $x_{1,2} = \pm L/2$. The right (+) and left (-) chiralities are denoted by right and left arrows.

III. DENSITY OF STATES OF A WIRE WITH TWO IMPURITIES - GENERAL FORM

The position dependent density of states can be obtained from the generalized retarded Green's function as follows:

$$\rho(x, \omega) = -\frac{1}{\pi} \sum_{r,r'} \text{Im}\{G_{r,r'}^R(x, x; \omega)\}, \quad (5)$$

where the retarded Green's function $G_{r,r'}^R(x, x'; \omega)$ is defined as the Fourier transform of:

$$G_{r,r'}^R(x, x'; t, t') = -i\Theta(t - t') \langle \{\psi_r(x, t); \psi_{r'}^\dagger(x', t')\} \rangle, \quad (6)$$

where Θ is the Heaviside function, and $\{a; b\}$ refers to the anticommutator.

In order to calculate the form of such Green's functions in the presence of impurities, we establish the Dyson equation associated to the Hamiltonian H . The details of the calculation are presented in Appendix A. Using the fact that Luttinger liquid chiral excitations are free to propagate in the presence of Coulomb interactions and considering the latter as strongly attenuated with distance, we obtain:

$$G_{r,r'}^R(x, x'; \omega) = g_r^R(x, x'; \omega) \delta_{r,r'} + \sum_{i=1,2} g_r^R(x, x_i; \omega) \times [\Gamma_i^B G_{-r,r'}^R(x_i, x'; \omega) + \Gamma_i^F G_{r,r'}^R(x_i, x'; \omega)], \quad (7)$$

where g_r^R are the Green's functions of a clean interacting homogeneous wire, associated to $H_0 + H_{\text{int}}$. They can be obtained in the framework of the Tomonaga-Luttinger theory.^{1,2} For an infinite QW with uniform interactions their form has been derived explicitly in Ref. 42. These Green's functions depend on a single chiral index r because the chiral states are eigenstates of the interacting QW in the absence of impurities:

$$g_r^R(x, x'; \omega) = \frac{-e^{irk_F(x-x')}}{2\hbar v_F \sqrt{\pi} \Gamma(1+\gamma)} \times \left(\frac{\omega_+}{\omega_c}\right) \left(\frac{2i|x-x'|\omega_c}{a\omega_+}\right)^{\frac{1}{2}-\gamma} \left[\mathbf{K}_{\gamma-\frac{1}{2}}\left(\frac{|x-x'|\omega_+}{ia\omega_c}\right) - \text{sgn}(r(x-x'))\mathbf{K}_{\gamma+\frac{1}{2}}\left(\frac{|x-x'|\omega_+}{ia\omega_c}\right)\right], \quad (8)$$

where $\omega_+ = \omega + i0$, k_F is the Fermi momentum, $\omega_c = v_F/a$, a is the small-distance cutoff of the Tomonaga-Luttinger liquid theory,^{1,2} Γ and \mathbf{K} are respectively the Gamma and modified Gamma functions, and $\gamma = (K + K^{-1} - 2)/4$. Here K is the interaction parameter which is related to the interaction potential by the relation $K = [1 + 4V(k \approx 0)/(\pi v_F)]^{-1/2}$. In the non-interacting limit, $K = 1$, Eq. (8) recovers the chiral Green's functions of a clean non-interacting QW:

$$g_r^R(x, x'; \omega) = -\frac{ie^{irk_F(x-x')}}{\hbar v_F} \times e^{i\omega r(x-x')/v_F} \Theta(r(x-x')). \quad (9)$$

From Eq. (7), we can extract the expressions of $G_{r,r}^R(x_i, x'; \omega)$ and $G_{-r,r}^R(x_i, x'; \omega)$ by solving a linear set of equations. We obtain (see Appendix B for the details of the calculation):

$$G_{r,r}^R(x_i, x'; \omega) = \frac{(1 - \chi_r^{ii})g_r^R(x_i, x'; \omega) + \chi_r^{ii}g_r^R(x_i, x'; \omega)}{(1 - \chi_r^{11})(1 - \chi_r^{22}) - \chi_r^{12}\chi_r^{21}}, \quad (10)$$

and,

$$\begin{aligned}
G_{-r,r}^R(x_i, x'; \omega) = & D^{-1} \sum_{j=1,2} g_{-r}^R(x_i, x_j; \omega) \Gamma_j^B G_{r,r}^R(x_j, x'; \omega) \\
& + D^{-1} \Gamma_i^B \Gamma_{\bar{i}}^F \left[g_{-r}^R(x_i, x_{\bar{i}}; \omega) g_{-r}^R(x_{\bar{i}}, x_i; \omega) \right. \\
& \left. - g_{-r}^R(x_i, x_i; \omega) g_{-r}^R(x_{\bar{i}}, x_{\bar{i}}; \omega) \right] G_{r,r}^R(x_i, x'; \omega), \quad (11)
\end{aligned}$$

with $\bar{i} = 1$ when $i = 2$, and $\bar{i} = 2$ when $i = 1$. Moreover, we have defined the quantities:

$$\begin{aligned}
D = & [1 - \Gamma_1^F g_{-r}^R(x_1, x_1; \omega)] [1 - \Gamma_2^F g_{-r}^R(x_2, x_2; \omega)] \\
& - \Gamma_1^F g_{-r}^R(x_1, x_2; \omega) \Gamma_2^F g_{-r}^R(x_2, x_1; \omega), \quad (12)
\end{aligned}$$

and,

$$\begin{aligned}
\chi_r^{ij} = & \Gamma_i^F g_r^R(x_i, x_j; \omega) \\
& + D^{-1} \left[\Gamma_1^B g_r^R(x_i, x_{\bar{j}}; \omega) \Gamma_2^B g_{-r}^R(x_{\bar{i}}, x_i; \omega) \right. \\
& + \Gamma_j^B g_r^R(x_i, x_j; \omega) \Gamma_{\bar{j}}^F g_{-r}^R(x_1, x_2; \omega) \Gamma_j^B g_{-r}^R(x_2, x_1; \omega) \\
& \left. + \Gamma_i^B g_r^R(x_i, x_j; \omega) \Gamma_{\bar{i}}^B g_{-r}^R(x_i, x_i; \omega) [1 - \Gamma_{\bar{j}}^F g_{-r}^R(x_{\bar{j}}, x_{\bar{j}}; \omega)] \right]. \quad (13)
\end{aligned}$$

The above formulas contain all the information necessary to calculate the LDOS of any chiral wire in the presence of one or two impurities as a function of energy and position. It is in fact a generalization of the solutions obtained in Ref. 43 for non-interacting systems to take into account the effects of interactions. An important improvement with respect to Ref. 43 is the fact that Eqs. (7), (10) and (11) are chirality resolved in order to include appropriately the Coulomb interactions.

In the following sections, we use these solutions to calculate the dependence of the density of states with energy and position for an infinite Luttinger liquid with different interaction strengths and impurity potentials, first for a QW with a single impurity (Sec. IV) and second, in the presence of two impurities (Sec. V).

IV. RESULTS FOR AN INFINITE SPINLESS LUTTINGER LIQUID WITH A SINGLE IMPURITY

In this section, we consider a QW with a single impurity located at position $x_1 = 0$. We can thus take $\Gamma_2^{F,B} = 0$, and Eq. (7) simplifies to:

$$\begin{aligned}
G_{r,r'}^R(x, x'; \omega) = & g_r^R(x, x'; \omega) \delta_{r,r'} + g_r^R(x, x_1; \omega) \\
& \times [\Gamma_1^B G_{-r,r'}^R(x_1, x'; \omega) + \Gamma_1^F G_{r,r'}^R(x_1, x'; \omega)]. \quad (14)
\end{aligned}$$

The details of solving the above Dyson equation are presented in Appendix C. We obtain:

$$\begin{aligned}
G_{r,r}^R(x_1, x'; \omega) = & g_r^R(x_1, x'; \omega) [1 - \Gamma_1^F g_{-r}^R(x_1, x_1; \omega)] \\
& \times [1 - \Gamma_1^F [g_r^R(x_1, x_1; \omega) + g_{-r}^R(x_1, x_1; \omega)] \\
& + g_r^R(x_1, x_1; \omega) [(\Gamma_1^F)^2 - (\Gamma_1^B)^2] g_{-r}^R(x_1, x_1; \omega)]^{-1}, \quad (15)
\end{aligned}$$

and,

$$G_{-r,r}^R(x_1, x'; \omega) = \frac{g_{-r}^R(x_1, x_1; \omega) \Gamma_1^B G_{r,r}^R(x_1, x'; \omega)}{1 - \Gamma_1^F g_{-r}^R(x_1, x_1; \omega)}. \quad (16)$$

This allows us to determine fully the LDOS.

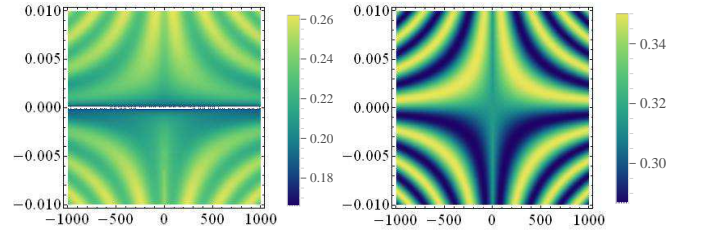


FIG. 2: LDOS (left graph) in the presence of Coulomb interactions ($K = 0.7$), and (right graph) for a non-interacting wire ($K = 1$) as a function of position (horizontal axis) and energy (vertical axis) for a weak impurity $\Gamma_1^{F,B} = 0.1\hbar\omega_c$. We take $k_F = 0$.

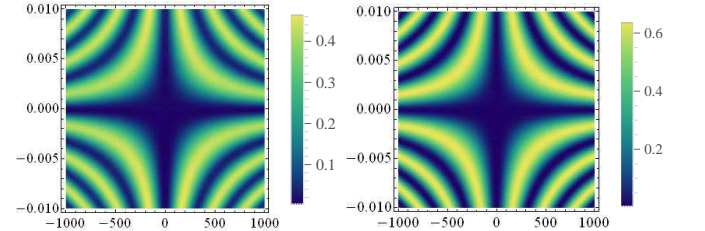


FIG. 3: The same as Fig. 2 for a strong impurity $\Gamma_1^{F,B} = 10\hbar\omega_c$.

In Figs. 2 and 3 we show the profiles of the LDOS for increasing impurity potential. While the LDOS is asymmetric in energy at weak impurity potential (Fig. 2), it becomes symmetrical for high impurity potential (Fig. 3). In addition, we observe a decreasing of the LDOS in the presence of interactions. As shown in Fig. 4 the amplitude of oscillations and the density of states at the impurity position are both reduced for $K = 0.7$ (left graph) in comparison to $K = 1$ (right graph).

The reduction of the LDOS at the impurity position (here $x_1 = 0$) when increasing the strength of the interactions is observed for all values of the impurity potential (see the left graph in Fig. 5). However, the LDOS

is drastically reduced for the largest impurity potentials for all values of K (black full line); this is because a large impurity effectively cuts the wire into two disconnected pieces.

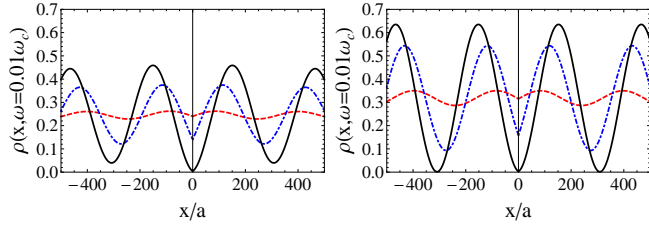


FIG. 4: LDOS in the presence of Coulomb interactions, $K = 0.7$ (left graph) and for a non-interacting wire, $K = 1$ (right graph) at $\omega = 0.01\omega_c$, and for $\Gamma_1^{F,B} = 0.1\hbar\omega_c$ (dashed red lines), $\Gamma_1^{F,B} = \hbar\omega_c$ (dash-dotted blue lines), and $\Gamma_1^{F,B} = 10\hbar\omega_c$ (solid black lines). We take $k_F = 0$.

In the right graph of Fig. 5 is shown the LDOS as a function of energy (on a logarithmic scale) for a position close to the impurity. For a weak impurity (red dashed line) the LDOS exhibits a power-law dependence with energy:

$$\rho_0(\omega) = \frac{|\omega|^{(K+K^{-1}-2)/2}}{\pi\Gamma\left(\frac{K+K^{-1}}{2}\right)}, \quad (17)$$

which is just the density of states of a clean interacting wire. Here Γ is the Gamma function. When the impurity potential increases, the LDOS deviates from this power law at small energy but converges and oscillates around this power law behavior when the energy increases, as expected (see the dash-dotted blue line and the black line). This behavior is in full agreement with the results obtained in Refs. 41 and 44. However, within our approach (and its limitations), we are not able to recover the expected behavior of the LDOS at low energy/distance and strong impurity potentials, i.e. a power law behavior of $|\omega|^{K^{-1}-1}$ characteristic to injecting an electron into the end of a semi-infinite wire. As detailed in the introduction we think that this is due to neglecting the Coulomb interactions between the electrons on the right and the left of the impurity.

It appears thus that this approximation will not influence the effect of the impurity on the behavior of the LDOS of an inhomogeneous wire for which one half would be non-interacting; we can thus expect to use our approach to accurately describe the physics of such an inhomogeneous wire for all energies and positions. Moreover we think that this approximation will have an effect only on the low-energy behavior, and that at high energy/large distances our results are valid even for the homogeneous interacting system. The range of validity of our approach depends on the impurity strength, the bulk power law being recovered for $|x| \gtrsim \hbar v_F / \Gamma^{F,B}$ and $|\hbar\omega| \gtrsim \Gamma^{F,B}$, i.e. when $|x\omega| \gtrsim v_F$.

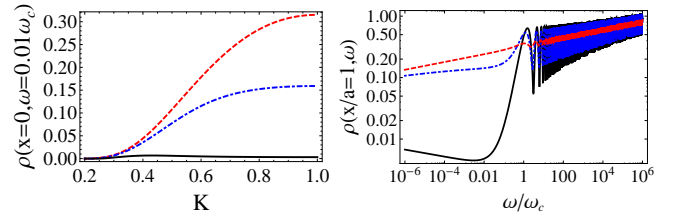


FIG. 5: LDOS (left graph) at the impurity position ($x = 0$) as a function of K , at $\omega = 0.01\omega_c$, and (right graph) close to the impurity position ($x/a = 1$) as a function of energy at $K = 0.7$. The right graph is plotted in a logarithm scale. On both graphs, we have $\Gamma_1^{F,B} = 0.01\hbar\omega_c$ (red dashed lines), $\Gamma_1^{F,B} = \hbar\omega_c$ (blue dash-dotted lines), and $\Gamma_1^{F,B} = 10\hbar\omega_c$ (black full lines). We take $k_F = 0$.

V. RESULTS FOR AN INFINITE SPINLESS LUTTINGER LIQUID WITH TWO IMPURITIES

In this section, we turn our interest to a QW with two impurities located at positions $x_{1,2} = \pm L/2$.

A. Density of states as a function of position and energy

We focus first on the analyse of the two-dimensional profiles of the LDOS as a function of position and energy. In Figs. 6, 7 and 8 we plot the profile of the density of states for increasing impurity potentials.

For small impurity potentials (see Fig. 6), we remark that the LDOS is odd in energy whereas it becomes even for strong impurity potentials (see Fig. 8), as it was the case for a single impurity. In the intermediate regime, the profile is neither odd, nor even (see Fig. 7). Moreover we note the evolution of the profiles from the weak-impurity Fabry-Perot regime to the strong-impurity, localized, Coulomb blockade regime.^{23,27,32,33} As previously shown for non-interacting systems, in the Fabry-Perot weak impurity regime the effect of the impurities reduces mostly to small sinusoidal oscillations of the LDOS with energy.⁴³ In the Coulomb blockade regime, the strong impurity potentials make the system evolve towards an isolated finite-size wire, whose LDOS is characterized by discrete energy levels, the distance between these levels being determined by the inverse length of the central part of the wire.^{29,30} As it can be seen from Figs. 6 to 8, these characteristics persist in the presence of interactions.

In fact, the profiles of the LDOS look qualitatively very similar between the interacting and non-interacting regimes. The main differences consist in a modification of the amplitude of the oscillations observed in the weak impurity regime, as well as in a modification of the height and width of the peaks observed in the strong impurity

regime. Small features corresponding to a power-law reduction of the LDOS close to zero energy in the interacting limit are also present, though they are not very visible in the two-dimensional profiles. To study these points quantitatively, in what follows we study separately the dependence of the LDOS on energy for a fixed position, as well as the dependence of the LDOS on the position for a given energy.

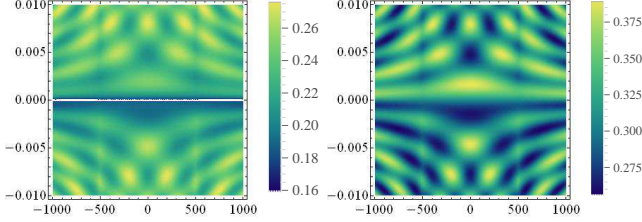


FIG. 6: LDOS (left graph) in the presence of Coulomb interactions ($K = 0.7$), and (right graph) for a non-interacting wire ($K = 1$) as a function of position (horizontal axis) and energy (vertical axis) for two symmetrical weak impurities $\Gamma_{1,2}^{F,B} = 0.1\hbar\omega_c$. The wire length is $L/a = 1000$, and we take $k_F = 0$.

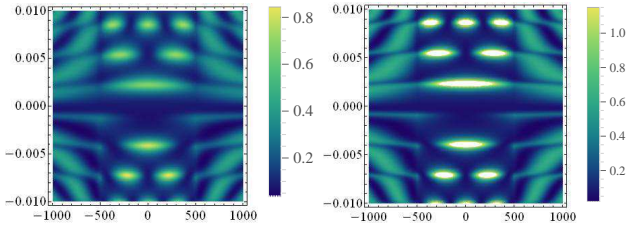


FIG. 7: The same as Fig. 6 for intermediate impurities $\Gamma_{1,2}^{F,B} = \hbar\omega_c$.

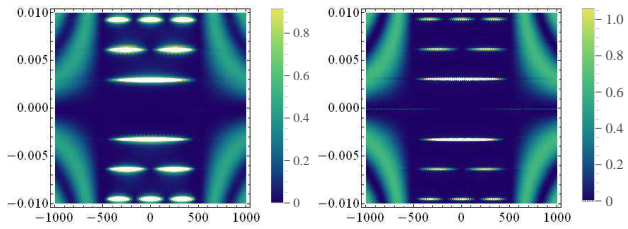


FIG. 8: The same as Fig. 6 for strong impurities $\Gamma_{1,2}^{F,B} = 10\hbar\omega_c$.

B. Density of states as a function of energy

Fig. 9 shows the density of states as a function of energy for two different positions: $x = 0$ (center of the wire) and $x = -L/4$ (halfway between the center of the wire and one impurity). For the interacting wire, in the weak

impurity regime (see dashed red lines), as expected for a Luttinger liquid, a power-law reduction of the LDOS can be observed close to $\omega = 0$. In the strong impurity regime (see solid black lines), as mentioned in the previous section, the central part of the wire is quasi-isolated and its spectrum resembles that of a finite size wire of length L which is characterized by discrete peaks with energies of $n\pi v_F/L$, with n being an integer. The height and width of the peaks depend on the coupling with the leads^{9,30} which explains the sharpening of the peaks with increasing the strength of the impurity potentials. Note that depending on the position x , some peaks may not appear in the spectrum. Indeed, as it can be seen also from Fig. 8, for $x = -L/4$, all the peaks are visible (see the solid black lines in the bottom graphs of Fig. 9) whereas for $x = 0$, only one peak out of two, corresponding to $\omega = (2n+1)\pi v_F/L$, is visible (see the solid black lines in the upper graphs of Fig. 9).

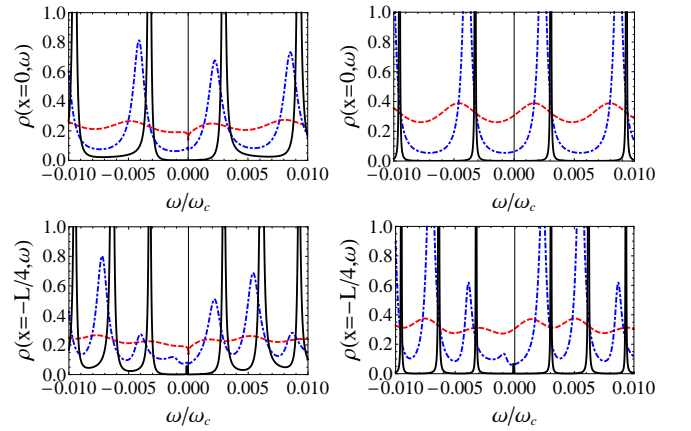


FIG. 9: LDOS (left graphs) in the presence of Coulomb interactions ($K = 0.7$) and for a non-interacting wire ($K = 1$) (right graphs) as a function of energy at two different positions, $x = 0$ (upper graphs) and $x = -L/4$ (bottom graphs), for $\Gamma_{1,2}^{F,B} = 0.1\hbar\omega_c$ (dashed red lines), $\Gamma_{1,2}^{F,B} = \hbar\omega_c$ (dash-dotted blue lines), and $\Gamma_{1,2}^{F,B} = 10\hbar\omega_c$ (solid black lines). We take $L/a = 1000$ and $k_F = 0$.

Also, as already mentioned in Secs. IV and V A, the parity with respect to energy changes with impurity strength both for interacting and non-interacting wires. To get some insight into these properties, we have performed a perturbative expansion of Eqs. (7) for $K = 1$. In the weak impurity regime, we find that the LDOS inside the wire can be written as:

$$\Delta\rho(x, \omega) = \rho_0 \sum_{i=1,1} \Gamma_i^B \sin\left(\frac{2\omega|x-x_i|}{v_F}\right), \quad (18)$$

with $\Delta\rho(x, \omega) = \rho(x, \omega) - \rho_0$, where ρ_0 is the density of states of the clean QW which takes a constant value for a non-interacting wire. This explains the odd parity of the LDOS described by the dashed red line in the upper right graph in Fig. 9. We note that in this regime the

impurity contribution to the LDOS is dominated by the backward scattering terms. The forward scattering does not play any role since the amplitudes Γ_1^F and Γ_2^F drop out from the asymptotic expression of Eq. (18). This is not the case in the strong impurity regime, for which we have found (not shown here) that the forward scattering terms are indispensable to recover the Coulomb blockade regime and cannot be neglected.

In order to understand how the effect of the Coulomb interactions affect the formation of the peaks in the LDOS, in Fig. 10 we plot the height and the width of the $\pi v_F/L$ peak as a function of K . When K decreases (i.e. when Coulomb interactions increase), the peak broadens and its height is reduced. Moreover the peak disappears completely for $K \lesssim 0.4$ and is replaced by an oscillating behavior of the LDOS. This result is quite intriguing as it would seem to indicate that, in what concerns the formation of the resonant levels, increasing the interactions effectively renormalizes the impurity strength to a smaller value, opposite to what would be intuitively expected from classical Luttinger-liquid arguments. Note that neither the distance between the peaks, nor their positions are affected by the interaction strength.

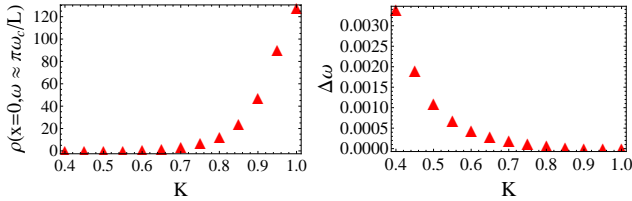


FIG. 10: Evolution of the peak amplitude (left graph) and peak width (right graph) as a function of K , for $\omega = \pi v_F/L$, $x = 0$, and $\Gamma_{1,2}^{F,B} = 10\hbar\omega_c$. We take $L/a = 1000$ and $k_F = 0$.

C. Density of states as a function of position

We focus now on the dependence of the LDOS on the position for a given energy (see Fig. 11). In the absence of interactions and in the strong impurity regime, the LDOS is uniformly zero in the wire for all energies that do not correspond to the formation of a peak (see the solid black line in the right graph), as expected (see Ref. 45). In the presence of interactions, this reduction is less apparent (see the solid black line in the left graph) due to a competition between the Coulomb interactions and the oscillatory behavior related to the presence of impurities. However, even in the presence of Coulomb interactions, the LDOS in the strong impurity regime is zero at the impurity positions $x = x_{1,2} = \pm L/2$, since in this regime the wire is effectively disconnected from the leads (see the solid black lines in Fig. 11).

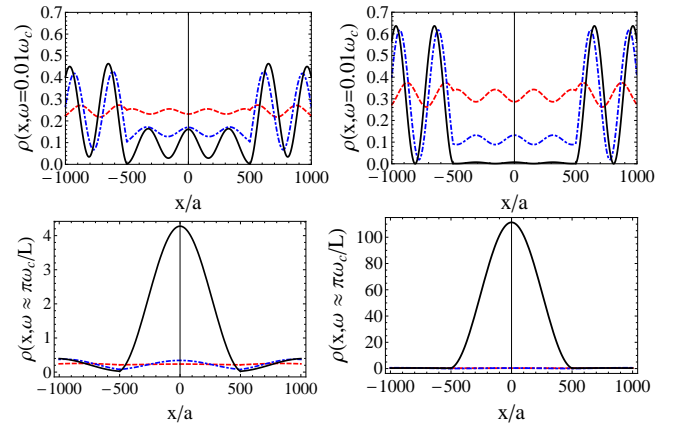


FIG. 11: LDOS for $K = 0.7$ (left graph) and $K = 1$ (right graph) as a function of position, for $\Gamma_{1,2}^{F,B} = 0.1\hbar\omega_c$ (dashed red lines), $\Gamma_{1,2}^{F,B} = \hbar\omega_c$ (dash-dotted blue lines), and $\Gamma_{1,2}^{F,B} = 10\hbar\omega_c$ (solid black lines). The energy is taken to be $\omega = 0.01\omega_c$ (upper graphs) and $\omega \approx \pi v_F/L$ (bottom graphs). We take $L/a = 1000$ and $k_F = 0$.

Last but not least, we consider the dependence of the LDOS as a function of position at $k_F \neq 0$. We are interested to compare our results with those of Ref. 37. In Fig. 12 we plot the LDOS as a function of position for $\omega = 0.01\omega_c$, and $k_F = 40\pi/L$ for an interacting wire $K = 0.7$ (left graph) and for a non-interacting wire $K = 1$ (right graph). Note that in the non-interacting QW the LDOS oscillates with a period of π/k_F , while in the interacting QW an extra modulation in the LDOS adds an envelope to the π/k_F oscillations, in agreement with Ref. 37. The period of this extra modulation is $\pi v_F/\omega$. Close to the impurities, the amplitude of oscillations does not decrease, contrary to what is obtained in Ref. 37. This discrepancy comes, as outlined above, from exiting the limits of the regime of validity of our approach when we approach the impurity positions. However, recovering the same extra modulation of the LDOS oscillations as those obtained in Ref. 37 using a completely different technique, gives us an additional confirmation of the validity of our method at high energies and large distances with respect to the impurities.

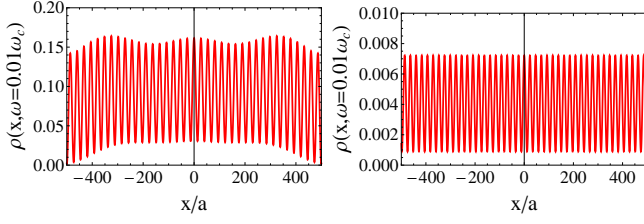


FIG. 12: LDOS for $x \in [-L/2, L/2]$, i.e. between the two impurities, in the presence of Coulomb interactions ($K = 0.7$) (left graph) and for a non-interacting wire ($K = 1$) (right graph) for $k_F = 40\pi/L$, $\Gamma_{1,2}^{F,B} = 10\hbar\omega_c$, and $\omega = 0.01\omega_c$. We take $L/a = 1000$.

VI. CONCLUSION

We have developed a new approach based on the Dyson equations which has allowed us to study the LDOS of an infinite interacting QW with two impurities of arbitrary strength. For an infinite homogeneous interacting wire with a single impurity we have calculated the form of the Friedel oscillations as well as the dependence of the LDOS with energy. We have found that for weak impurities, as well as for strong impurities at high energies/large distances, our approach recovers the expected Luttinger liquid power-law dependence; however it breaks down for strong impurities at low energy/small distance.

We have applied this approach to study the transition from the weak-impurity regime to the strong-impurity regime in a wire with two impurities, focusing in particular on the regime of large distances and energies. We have found that the main effect of interactions is to reduce the amplitude of the Fabry-Perot oscillations in the weak impurity limit, as well as of the Coulomb blockade peaks in the strong impurity limit. The interactions do not affect the periodicity of the oscillations, neither the distance between the peaks. Moreover, we see that strong interactions also reduce to zero the LDOS on the impurity sites. Also, at non-zero k_F and for strong impurities our results are consistent with those obtained in Ref. 37 for the LDOS of a Luttinger liquid in a box, in particular we recover an extra modulation of the LDOS oscillations in the presence of interactions, which is absent in the non-interacting system. This provides us with an extra confirmation that our approach is valid in this regime.

We believe that the low-energy discrepancies between our results and the ones predicted by the perturbation theory in the strong impurity limit arise from neglecting the interactions between the electrons on the right and on the left of the impurities. To improve this approximation we plan in the future to focus on an inhomogeneous wire made of a central interacting region and two semi-infinite non-interacting leads, for which such terms would be absent. Our method is very general and can be easily applied to such a

system. We can also generalize our approach to take into account other factors such as the electronic spin which will allow us to characterize more realistic system. We believe that our work provides an important first step in constructing a novel non-perturbative approach to understand the interplay between interactions and arbitrary size-impurities in one-dimensional systems.

Acknowledgements

We would like to thank Julia Meyer and Pascal Simon for interesting discussions. The work of C.B. and M.G. is supported by the ERC Starting Independent Researcher Grant NANOGAPHENE 256965.

Appendix A: Derivation of the Dyson equation

To establish the Dyson equation for the retarded Green's function defined in Eq. (6), we evaluate $\partial_t \psi_r(x, t) = i[H; \psi_r(x, t)]/\hbar$, where $[a; b]$ denotes the commutator. We obtain:

$$\begin{aligned} \partial_t \psi_r(x, t) &= r v_F \partial_x \psi_r(x, t) \\ &- \frac{i}{\hbar} \sum_{i=1,2} [\lambda_i^B(x) \psi_{-r}(x, t) + \lambda_i^F(x) \psi_r(x, t)] \\ &- \frac{i}{2\hbar} \sum_{r_1, r_2, r_3} \int_{-\infty}^{\infty} dx'' V(x, x'') \\ &\times \left\{ \psi_{r_1}^\dagger(x'', t) \psi_{r_2}(x'', t); \psi_{r_3}(x, t) \right\}. \end{aligned} \quad (A1)$$

Notice that the last term, which corresponds to the Coulomb interactions contribution, does not depend on r since the interactions act similarly on both chiralities. After multiplying by the operator $\psi_{r'}^\dagger(x', t')$, we get:

$$\begin{aligned} \partial_t \psi_r(x, t) \psi_{r'}^\dagger(x', t') &= r v_F \partial_x \psi_r(x, t) \psi_{r'}^\dagger(x', t') \\ &- \frac{i}{\hbar} \sum_{i=1,2} \lambda_i^B(x) \psi_{-r}(x, t) \psi_{r'}^\dagger(x', t') \\ &- \frac{i}{\hbar} \sum_{i=1,2} \lambda_i^F(x) \psi_r(x, t) \psi_{r'}^\dagger(x', t') \\ &- \frac{i}{2\hbar} \sum_{r_1, r_2, r_3} \int_{-\infty}^{\infty} dx'' V(x, x'') \\ &\times \left[\psi_{r_1}^\dagger(x'', t) \psi_{r_2}(x'', t) \psi_{r_3}(x, t) \psi_{r'}^\dagger(x', t') \right. \\ &\left. + \psi_{r_3}(x, t) \psi_{r_1}^\dagger(x'', t) \psi_{r_2}(x'', t) \psi_{r'}^\dagger(x', t') \right]. \end{aligned} \quad (A2)$$

Making the assumption that the Coulomb potential $V(x, x'')$ decreases when the distance $x - x''$ increases, we keep only the dominant part in the integrals over x'' ,

i.e., the $x \approx x''$ contribution, thus:

$$\begin{aligned}
& \partial_t \psi_r(x, t) \psi_{r'}^\dagger(x', t') = rv_F \partial_x \psi_r(x, t) \psi_{r'}^\dagger(x', t') \\
& - \frac{i}{\hbar} \sum_{i=1,2} \lambda_i^B(x) \psi_{-r}(x, t) \psi_{r'}^\dagger(x', t') \\
& - \frac{i}{\hbar} \sum_{i=1,2} \lambda_i^F(x) \psi_r(x, t) \psi_{r'}^\dagger(x', t') \\
& - \frac{i}{2\hbar} \sum_{r_1, r_2, r_3} V(x, x) \\
& \times \left[\psi_{r_1}^\dagger(x, t) \psi_{r_2}(x, t) \psi_{r_3}(x, t) \psi_{r'}^\dagger(x', t') \right. \\
& \left. + \psi_{r_3}(x, t) \psi_{r_1}^\dagger(x, t) \psi_{r_2}(x, t) \psi_{r'}^\dagger(x', t') \right], \quad (\text{A3})
\end{aligned}$$

which reduces to:

$$\begin{aligned}
& \partial_t \psi_r(x, t) \psi_{r'}^\dagger(x', t') = rv_F \partial_x \psi_r(x, t) \psi_{r'}^\dagger(x', t') \\
& - \frac{i}{\hbar} \sum_{i=1,2} \lambda_i^B(x) \psi_{-r}(x, t) \psi_{r'}^\dagger(x', t') \\
& - \frac{i}{\hbar} \sum_{i=1,2} \lambda_i^F(x) \psi_r(x, t) \psi_{r'}^\dagger(x', t') \\
& - \frac{i}{\hbar} V_0 \sum_{r_1} \psi_{r_1}(x, t) \psi_{r'}^\dagger(x', t'), \quad (\text{A4})
\end{aligned}$$

since there is a compensation of terms when one sums over r_2 and r_3 . We have introduced $V_0 = V(x, x)$. We can show in a similar manner that:

$$\begin{aligned}
& \psi_{r'}^\dagger(x', t') \partial_t \psi_r(x, t) = rv_F \psi_{r'}^\dagger(x', t') \partial_x \psi_r(x, t) \\
& - \frac{i}{\hbar} \sum_{i=1,2} \lambda_i^B(x) \psi_{r'}^\dagger(x', t') \psi_{-r}(x, t) \\
& - \frac{i}{\hbar} \sum_{i=1,2} \lambda_i^F(x) \psi_{r'}^\dagger(x', t') \psi_r(x, t) \\
& - \frac{i}{\hbar} V_0 \sum_{r_1} \psi_{r'}^\dagger(x', t') \psi_{r_1}(x, t). \quad (\text{A5})
\end{aligned}$$

Taking the time derivative of Eq. (6):

$$\begin{aligned}
& i\partial_t G_{r,r'}^R(x, x'; t, t') = \delta_{r,r'} \delta(x - x') \delta(t - t') \\
& + \Theta(t - t') \langle \{ \partial_t \psi_r(x, t); \psi_{r'}^\dagger(x', t') \} \rangle, \quad (\text{A6})
\end{aligned}$$

and substituting Eqs. (A4) and (A5) in Eq. (A6), we obtain:

$$\begin{aligned}
& (i\hbar \partial_t - irv_F \partial_x - V_0) G_{r,r'}^R(x, x'; t, t') = \\
& \delta_{r,r'} \delta(x - x') \delta(t - t') \\
& + \sum_{i=1,2} \left[\lambda_i^B(x) G_{-r,r'}^R(x, x'; t, t') \right. \\
& \left. + \lambda_i^F(x) G_{r,r'}^R(x, x'; t, t') \right], \quad (\text{A7})
\end{aligned}$$

where we have neglected the contribution involving distinct chiralities in the interacting term since in a Luttinger liquid, chiral excitations are free to propagate (no mixing of chiralities due to interactions).

Performing the integrals over space and time, and introducing the Green's functions of the clean interacting wire described by $H_0 + H_{\text{int}}$, g_r^R , which obey the equation of motion:

$$(i\hbar \partial_t - irv_F \partial_x - V_0) g_r^R(x, x'; t, t') = \delta(x - x') \delta(t - t'), \quad (\text{A8})$$

we end up with:

$$\begin{aligned}
G_{r,r'}^R(x, x'; t, t') &= g_r^R(x, x'; t, t') \delta_{r,r'} \\
&+ \sum_{i=1,2} \int dt'' \int dx'' g_r^R(x, x''; t, t'') \\
&\times [\lambda_i^B(x'') G_{-r,r'}^R(x'', x'; t'', t') \\
&+ \lambda_i^F(x'') G_{r,r'}^R(x'', x'; t'', t')] , \quad (\text{A9})
\end{aligned}$$

which leads, after a Fourier transform, to Eq. (7), if we assume delta-function localized impurities, i.e., $\lambda_i^{F,B}(x) = \Gamma_i^{F,B} \delta(x - x_i)$ for $i = 1, 2$. Notice that the Coulomb potential V_0 does not appear explicitly in Eq. (A9) because it has been incorporated in the Green's function of the clean wire, g_r^R (see Eq. (A8)).

Appendix B: Solution of the Dyson equation for two impurities

By taking first, $x = x_1$, and second, $x = x_2$, in Eq. (7) with $r = \pm r'$, we obtain a set of linear coupled equations (all the frequency arguments have been dropped in order to simplify the notations):

$$\begin{aligned}
G_{r,r}^R(x_1, x') &= g_r^R(x_1, x') \\
&+ g_r^R(x_1, x_1) \Gamma_1^B G_{-r,r}^R(x_1, x') \\
&+ g_r^R(x_1, x_2) \Gamma_2^B G_{-r,r}^R(x_2, x') \\
&+ g_r^R(x_1, x_1) \Gamma_1^F G_{r,r}^R(x_1, x') \\
&+ g_r^R(x_1, x_2) \Gamma_2^F G_{r,r}^R(x_2, x'), \quad (\text{B1})
\end{aligned}$$

$$\begin{aligned}
G_{r,r}^R(x_2, x') &= g_r^R(x_2, x') \\
&+ g_r^R(x_2, x_1) \Gamma_1^B G_{-r,r}^R(x_1, x') \\
&+ g_r^R(x_2, x_2) \Gamma_2^B G_{-r,r}^R(x_2, x') \\
&+ g_r^R(x_2, x_1) \Gamma_1^F G_{r,r}^R(x_1, x') \\
&+ g_r^R(x_2, x_2) \Gamma_2^F G_{r,r}^R(x_2, x'), \quad (\text{B2})
\end{aligned}$$

and,

$$\begin{aligned}
G_{-r,r}^R(x_1, x') &= g_{-r}^R(x_1, x_1) \Gamma_1^B G_{r,r}^R(x_1, x') \\
&+ g_{-r}^R(x_1, x_2) \Gamma_2^B G_{r,r}^R(x_2, x') \\
&+ g_{-r}^R(x_1, x_1) \Gamma_1^F G_{-r,r}^R(x_1, x') \\
&+ g_{-r}^R(x_1, x_2) \Gamma_2^F G_{-r,r}^R(x_2, x'), \quad (\text{B3})
\end{aligned}$$

$$\begin{aligned}
G_{-r,r}^R(x_2, x') &= g_{-r}^R(x_2, x_1) \Gamma_1^B G_{r,r}^R(x_1, x') \\
&+ g_{-r}^R(x_2, x_2) \Gamma_2^B G_{r,r}^R(x_2, x') \\
&+ g_{-r}^R(x_2, x_1) \Gamma_1^F G_{-r,r}^R(x_1, x') \\
&+ g_{-r}^R(x_2, x_2) \Gamma_2^F G_{-r,r}^R(x_2, x') . \quad (B4)
\end{aligned}$$

From Eqs. (B3) and (B4), we extract the expressions of $G_{-r,r}^R$ and express them only in terms of the Green's functions $G_{r,r}^R$. Thus we get:

$$\begin{aligned}
G_{-r,r}^R(x_1, x') &= D^{-1} \sum_{j=1,2} g_{-r}^R(x_1, x_j) \Gamma_j^B G_{r,r}^R(x_j, x') \\
&+ D^{-1} \Gamma_1^B \Gamma_2^F \left[g_{-r}^R(x_1, x_2) g_{-r}^R(x_2, x_1) \right. \\
&\quad \left. - g_{-r}^R(x_1, x_1) g_{-r}^R(x_2, x_2) \right] G_{r,r}^R(x_1, x') , \quad (B5)
\end{aligned}$$

and,

$$\begin{aligned}
G_{-r,r}^R(x_2, x') &= D^{-1} \sum_{j=1,2} g_{-r}^R(x_2, x_j) \Gamma_j^B G_{r,r}^R(x_j, x') \\
&+ D^{-1} \Gamma_2^B \Gamma_1^F \left[g_{-r}^R(x_2, x_1) g_{-r}^R(x_1, x_2) \right. \\
&\quad \left. - g_{-r}^R(x_2, x_2) g_{-r}^R(x_1, x_1) \right] G_{r,r}^R(x_2, x') , \quad (B6)
\end{aligned}$$

where D is defined by Eq. (12). Eqs. (B5) and (B6) correspond to Eq. (11). Next, substituting Eqs. (B5) and (B6) in Eqs. (B1) and (B2), we end up with a system of two linear equations whose solutions are:

$$G_{r,r}^R(x_1, x'; \omega) = \frac{(1 - \chi_r^{22}) g_r^R(x_1, x'; \omega) + \chi_r^{12} g_r^R(x_2, x'; \omega)}{(1 - \chi_r^{11})(1 - \chi_r^{22}) - \chi_r^{12} \chi_r^{21}} , \quad (B7)$$

and,

$$G_{r,r}^R(x_2, x'; \omega) = \frac{(1 - \chi_r^{11}) g_r^R(x_2, x'; \omega) + \chi_r^{21} g_r^R(x_1, x'; \omega)}{(1 - \chi_r^{11})(1 - \chi_r^{22}) - \chi_r^{12} \chi_r^{21}} ,$$

where χ_r^{ij} is defined by Eq. (13). Eqs. (B7) and (B8) correspond to Eq. (10).

Appendix C: Solution of the Dyson equation for a single impurity

We consider a single impurity located at position x_1 . In that case $\Gamma_2^B = \Gamma_2^F = 0$ and Eq. (A9) simplifies. After a Fourier transform, we obtain:

$$\begin{aligned}
G_{r,r'}^R(x, x'; \omega) &= g_r^R(x, x'; \omega) \delta_{r,r'} + g_r^R(x, x_1; \omega) \\
&\times [\Gamma_1^B G_{-r,r'}^R(x_1, x'; \omega) + \Gamma_1^F G_{r,r'}^R(x_1, x'; \omega)] . \quad (C1)
\end{aligned}$$

We can extract the expressions of $G_{r,r}^R(x_1, x'; \omega)$ and $G_{-r,r}^R(x_1, x'; \omega)$ by solving a linear set of equations as done in Appendix B. We obtain:

$$G_{r,r}^R(x_1, x'; \omega) = \frac{g_r^R(x_1, x'; \omega)}{1 - \chi_r^{11}} , \quad (C2)$$

and,

$$G_{-r,r}^R(x_1, x'; \omega) = \frac{g_{-r}^R(x_1, x_1; \omega) \Gamma_1^B G_{r,r}^R(x_1, x'; \omega)}{1 - \Gamma_1^F g_{-r}^R(x_1, x_1; \omega)} , \quad (C3)$$

where χ_r^{11} for a single impurity reduces to:

$$\begin{aligned}
\chi_r^{11} &= \Gamma_1^F g_r^R(x_1, x_1; \omega) \\
&+ \frac{g_r^R(x_1, x_1; \omega) (\Gamma_1^B)^2 g_{-r}^R(x_1, x_1; \omega)}{1 - \Gamma_1^F g_{-r}^R(x_1, x_1; \omega)} . \quad (C4)
\end{aligned}$$

Replacing Eq. (C4) in Eqs. (C2) and (C3), we end up (B8) with Eqs. (15) and (16).

¹ S. Tomonaga, Prog. Theor. Phys **5**, 544 (1950).

² J.M. Luttinger, J. Math. Phys. **4**, 1154 (1963).

³ D.C. Mattis and E.H. Lieb, J. Math. Phys. **6**, 304 (1965).

⁴ F.D.M. Haldane, J. Phys. C **14**, 2585 (1981).

⁵ A.O. Gogolin, A.A. Nersisyan, and A.M. Tsvelik, in *Bosonization and Strongly Correlated Systems* (Cambridge University Press, Cambridge, 1998).

⁶ L.I. Glazman, I.M. Ruzin, and B.I. Shklovskii, Phys. Rev. B **45**, 8454 (1992).

⁷ C.L. Kane and M.P.A. Fisher, Phys. Rev. B **46**, 15233 (1992).

⁸ C.L. Kane and M.P.A. Fisher, Phys. Rev. Lett. **68**, 1220 (1992).

⁹ M.P.A. Fisher and L.I. Glazman, in *Mesoscopic Electron Transport*, NATO ASI, edited by L. Kouwenhoven, G. Schon, and L. Sohn (Kluwer, Dordrecht, 1997), Vol. 345, p. 331.

¹⁰ D.L. Maslov, Phys. Rev. B **52**, R14368 (1995).

¹¹ M. Fabrizio and A.O. Gogolin, Phys. Rev. Lett. **78**, 4527 (1997).

¹² R. Egger and H. Grabert, Phys. Rev. B **58**, 10761 (1998).

¹³ F. Dolcini, H. Grabert, I. Safi, and B. Trauzettel, Phys. Rev. Lett. **91**, 266402 (2003).

¹⁴ F. Dolcini, B. Trauzettel, I. Safi, and H. Grabert, Phys. Rev. B **71**, 165309 (2005).

¹⁵ W. Metzner, M. Salmhofer, C. Honerkamp, V. Meden, and

- K. Schoenhammer, Rev. Mod. Phys. **84**, 299 (2012).
- ¹⁶ P. Fendley, A.W.W. Ludwig, and H. Saleur, Phys. Rev. B **52**, 8934 (1995); Phys. Rev. Lett. **75**, 2196 (1995).
 - ¹⁷ W. Liang, M. Bockrath, D. Bozovic, J. H. Hafner, M. Tinkham, and H. Park, Nature (London), **411**, 665 (2001).
 - ¹⁸ C. Bena, S. Vishveshwara, L. Balents, and M. P. A. Fisher, J. Stat. Phys. **103**, 429 (2001).
 - ¹⁹ B. Trauzettel, I. Safi, F. Dolcini, and H. Grabert, Phys. Rev. Lett. **92**, 226405 (2004).
 - ²⁰ I. Safi, C. Bena, and A. Crépieux, Phys. Rev. B **78**, 205422 (2008).
 - ²¹ A. Crépieux, R. Guyon, P. Devillard, and T. Martin, Phys. Rev. B **67**, 205408 (2003); A.V. Lebedev, A. Crépieux, and T. Martin, *ibid.* **71**, 075416 (2005); M. Guigou, A. Popoff, T. Martin, and A. Crépieux, *ibid.* **76**, 045104 (2007).
 - ²² P. Recher, N.Y. Kim, and Y. Yamamoto, Phys. Rev. B **74**, 235438 (2006).
 - ²³ N.Y. Kim, P. Recher, W. D. Oliver, Y. Yamamoto, J. Kong, and H. Dai, Phys. Rev. Lett. **99**, 036802 (2007).
 - ²⁴ L.G. Herrmann, T. Delattre, P. Morfin, J.-M. Berroir, B. Plaças, D.C. Glattli, and T. Kontos, Phys. Rev. Lett. **99**, 156804 (2007).
 - ²⁵ I. Safi and H. Schulz, Phys. Rev. B **52**, R17040 (1995); D. Maslov and M. Stone, *ibid.* **52**, R5539 (1995); V.V. Ponomarenko, *ibid.* **52**, R8666 (1995).
 - ²⁶ F. Wu, P. Queipo, A. Nasibulin, T. Tsuneta, T.H. Wang, E. Kauppinen, and P.J. Hakonen, Phys. Rev. Lett. **99**, 156803 (2007); P.-E. Roche, M. Kociak, S. Guéron, A. Kasumov, B. Reulet, and H. Bouchiat, Eur. Phys. J. B **28**, 217 (2002).
 - ²⁷ M. Bockrath, D.H. Cobden, J. Lu, A.G. Rinzler, R.E. Smalley, L. Balents, and P.L. McEuen, Nature **397**, 598 (1999).
 - ²⁸ Z. Yao, H.W.Ch. Postma, L. Balents, and C. Dekker, Nature **402**, 273 (1999).
 - ²⁹ S.J. Tans, M.H. Devoret, R.J.A. Groeneveld, and C. Dekker, Nature **394**, 761 (1998).
 - ³⁰ M. Bockrath, D.H. Cobden, P.L. McEuen, N.G. Chopra, A. Zettl, A. Thess, and R.E. Smalley, Science **275**, 1922 (1997).
 - ³¹ J. Nygard, D.H. Cobden, M. Bockrath, P.L. McEuen, and P.E. Lindelof, App. Phys. A **69**, 297 (1999).
 - ³² W. Liang, M. Bockrath, and H. Park, Phys. Rev. Lett. **88**, 126801 (2002).
 - ³³ A. Rubio, S.A. Apell, L.C. Venema and C. Dekker, Eur. Phys. J. B **17**, 301 (2000).
 - ³⁴ C.S. Peca, L. Balents, and K.J. Wiese, Phys. Rev. B **68**, 205423 (2003).
 - ³⁵ J. Alicea, C. Bena, L. Balents, and M.P.A. Fisher, Phys. Rev. B **69**, 155332 (2004).
 - ³⁶ R. Zamoum, M. Guigou, C. Bena, and A. Crépieux, in preparation.
 - ³⁷ F. Anfuso and S. Eggert, Phys. Rev. B **68**, 241301R (2003).
 - ³⁸ Y. Oreg and A.M. Finkel'stein, Phys. Rev. Lett. **76**, 4230 (1996).
 - ³⁹ A. Furusaki, Phys. Rev. B **56**, 9352 (1997).
 - ⁴⁰ J. von Delft and H. Schoeller, Annalen Phys. **7**, 225 (1998).
 - ⁴¹ A. Grishin, I.V. Yurkevich, and I.V. Lerner, Phys. Rev. B **69**, 165108 (2004).
 - ⁴² B. Braunecker, C. Bena, and P. Simon, Phys. Rev. B **85**, 035136 (2012).
 - ⁴³ X.L. Song, Z.Y. Zhao, Y. Wang, and Y.M. Shi, Jour. of Shanghai university, 7(4), **361** (2003).
 - ⁴⁴ S. Eggert, H. Johannesson, and A. Mattsson, Phys. Rev. Lett. **76**, 1505 (1996).
 - ⁴⁵ V.A. Sablikov, S.V. Polyakov, and M. Büttiker, Phys. Rev. B **61**, 13763 (2000).